ROBOMECH Journal

RESEARCH ARTICLE

Open Access

Development of a steerable in-pipe locomotive device with six braided tubes

Hirozumi Takeshima[1*] and Toshio Takayama[2]

Abstract

Numerous studies have developed in-pipe locomotive devices to inspect pipes. However, it is difficult to achieve selective locomotion in a branched piping system. In this study, a novel steerable in-pipe locomotive device is proposed based on "a six-braided-tubes locomotive device," which is an in-pipe locomotive device that is actuated by only six pneumatic inflatable tubes. It is one of the simplest in-pipe locomotive devices that is capable of forward and backward motion and can rotate in clockwise and counterclockwise directions along a pipe, can select the desired pathway in the branched pipe. In this paper, we discuss the background of pipe inspection, classify previously developed in-pipe locomotive devices, and clarify the aim of this study. Additionally, we also describe and extend the locomotive principles of six-braided-tubes locomotive devices. Moreover, we propose a novel attachment, termed steering hook, to enable steering in various types of branched systems. Finally, we experimentally confirm that the novel proposed principle allows the device to correct path selection in an in-pipe branched piping system.

Keywords: Soft robotics, Pneumatic system, In-pipe locomotive device, In-pipe path-selection

Objective

Piping does not only include industrial gas and liquid pipes, but also blood vessels and organs, as they also need to achieve efficient transfer or flow of fluids. It is important to inspect and maintain these systems to ensure good performance.

There are many nondestructive inspection technologies [1]. Some of them have been applied for the external inspection of pipes. X-ray [2] employs radiography for interior pipe visualization, whereas ultrasound [3] and eddy current techniques [4] measure the thickness of a pipe. These technologies are not only applied in industrial fields, but also in the field of medicine, as X-ray, ultrasound, and magnetic resonance imaging (MRI) are utilized to perform health screenings.

However, there are many piping systems that cannot be inspected from the outside, as they are located within a wall or underground, obstructed by various obstacles. Moreover, the above-mentioned external inspection techniques may yield undesirable effects on the piping, or can be rendered ineffective because of the physical characteristics of the pipes. For example, radiation exposure is a consequence of X-ray inspection, and non-conductive materials cannot be inspected with an eddy current. Since endoscopes enable the maintenance and inspection of pipes without disassembly, and allow visual inspection of piping regardless of its location and material, they have become widely utilized in studies on pipe inspection technology. Although there are certain types of pipes in which it is difficult to insert an endoscope, such as long, narrow, or bent pipes, there are many studies on in-pipe locomotive devices that facilitate endoscope operation in such difficult pipes.

Most in-pipe locomotive devices can be classified as one of the following: a wheeled or crawler device, an inchworm device, or a walking device equipped with legs or leads.

Wheeled and crawler devices have a long history of use [5, 6] and have the advantage of reaching speeds that are higher than those employing other propulsion techniques. However, these types of devices not only require a mechanism to ensure continuous rotation, but also a mechanism that generates a propulsion force of friction

*Correspondence: takeshima.h.aa@m.titech.ac.jp
[1] Tokyo Institute of Technology, 4259, Nagatsutacho, Midori-ku, Yokohama-shi, Kanagawa 226-0026, Japan
Full list of author information is available at the end of the article

by pushing wheels or crawlers to an inner wall of a piping [7–10], thereby increasing design complexity. Thus, for simplification, several researchers have adopted the use of a mechanical spring to push wheels or crawlers to an inner wall and generate friction [11–13]. Additionally, Kataoka et al. [14] developed a device that utilizes highly elastic crawlers, and Zin et al. [15] developed a device that uses magnetic force to adhere to the inner wall of pipes.

Alternatively, the structure of inchworm devices is much simpler than that of wheeled devices or crawlers [16, 17]. To further reduce the design complexity, several researchers have adopted the use of fluid power to drive the devices [18–24]. Other propulsion methods for in-pipe locomotive devices include wave-like propulsion [25] and multi-gait walking [26–28].

Some piping systems have a branched part. Therefore, in-pipe locomotive devices must be able to travel forward and backward, and turn to proceed into a branched pipe. Because of this requirement, many researchers have focused on the realization of a steerable in-pipe device. For example, locomotive devices purposed for travelling through 200-mm-diameter pipes have been equipped with separate motors for locomotion, rotation, and steering [10, 13, 17]. To simplify the design and reduce the number of motors, Nishimura et al. [11] proposed a differential mechanism that allows locomotion, rotation, and steering to be realized with only two motors. Debenest et al. [12] designed a spring mechanism to eliminate the need of a separate motor to control steering. Additionally, a steering mechanism has been included in certain inchworm devices to enable path selection in branched piping systems. This type of steering component has three or four degrees of freedom (DoFs), and is typically attached at the tip of the device [23, 24].

Most of the above-mentioned devices are equipped separately with a basic travel mechanism and a steering mechanism to enable path selection in branched piping systems. However, the added steering mechanism increases device complexity, and prevents the device from being small and affordable. Thus, in this paper, we propose the use of a bundled-tube device for the development of a simple and affordable steerable in-pipe robotic device. A bundled-tube device is a novel in-pipe robot with inflatable tubes, which we have described in a previous study [29]; unlike other similarly purposed devices, our bundled-tube device utilizes snake-like motion to travel. This snake-like motion, which is based on bending motion, has previously been utilized by rigid multi-DoF snake robots [30]. Although our device only comprises inflatable braided tubes and has a simple structure, it can use snake-like motion to travel through pipes. More specifically, forward movement through a pipe is driven by periodic inflation and deflation of each of the tubes, whereas backward movement is achieved by applying an opposing pressurization pattern to the device. Additionally, the entire body of this bundled-tube device is quite soft and generates a propulsion force; hence, it can travel along curved sections and sections with dynamically changing diameter and shapes. The soft body allows the device to conform to the shape of a pipe by exploiting the reaction force from the pipe; furthermore, a propulsion force, which is generated by the inserted entire body, can easily overcome the force of friction, which is generated by travelling through curved sections and increased by an increment of the insertion length. Moreover, the simple structure of the bundled-tube device allows the cable that follows the pipe inspection module, such as an electric wire and an optical fiber, to become a locomotive device when attached to bundled tubes around the cable. Therefore, more stable and robust locomotion can be achieved by surrounding all of the cables with a bundled-tube locomotive device. Previously, we have developed several types of such bundled-tube devices, including a helical-type device [31], a three-braided tube device [32], and six braided-tube device [33].

A six braided-tube device (Fig. 1) comprises three tubes that form right-handed helices (Fig. 1b) and three tubes that form left-handed helices (Fig. 1c). Tubes of both groups are braided around a nonstretchable thread. As previously described, the forward movement is driven by the periodic inflation and deflation of each of the tubes. In the previous work [31], we describe a mechanical principle of a braided tube device, and discovered that an

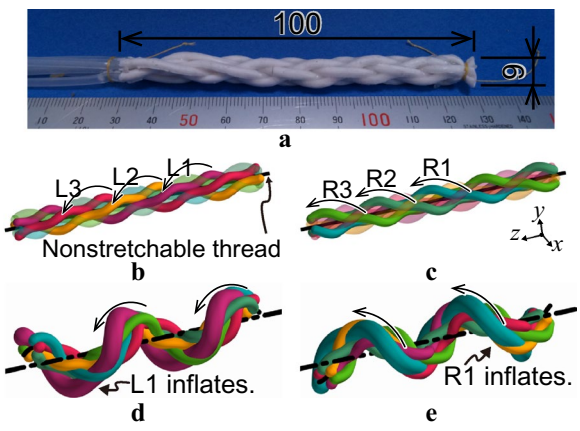

Fig. 1 Six braided-tube in-pipe locomotive device. Group R tubes form the right-handed helices, and Group L tubes form the left-handed helices. **a** is an appearance of a device. **b**, **c** are Group L and R tubes, respectively. **d**, **e** Deformations with an inflation with a left- and right-handed tubes. A left- and right-handed tubes deforms a device into right- and left-handed helices, respectively

inflation of a helical tube placed around a nonstretchable thread bends a device into a same direction helix. Specifically, the six-tube device can deform into a left- and right-handed helix with a left- and right-handed helical tube (Fig. 1d, e). A combination of both directions of the tubes enables the six tubes to independently control the locomotion and rotation of the device.

This study aims to employ this novel six braided-tube locomotion strategy for propulsion, rotation, and steering in piping systems. The ability of the proposed device to control its position and orientation will enable it to perform path selection in branched piping systems without the need of a complicated attachment or additional actuators, thereby making it one of the simplest in-pipe locomotive devices able to achieve path selection. In this chapter, we introduced and described previous studies and the aim of this study. In Chapter 2, we will introduce the fundamental principles of six-braided tube locomotion. Based on the fundamental principles, we propose a novel locomotive method and an accompanying strategy for path selection. We also propose a simple and tiny attachment referred to as a steering hook, which is required for the device to select the correct path in branched piping systems. Chapter 3 describes the characteristics of prototypes and the experimental equipment. Then, the experimental results, which are presented in Chapter 4, confirm the ability of a six-braided tube device to perform path selection. Finally, the conclusions of this study are outlined in Chapter 5.

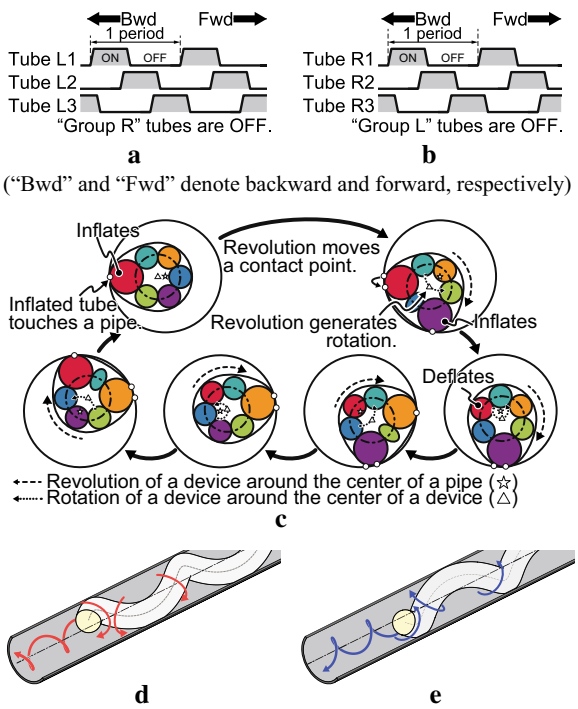

Fig. 2 Motion of six braided-tube device in the case of driving only one group. Periodical pressurizations generate a revolution of a device around a center of a pipe and a rotation of a device around a center of a device. **a** and **b** Pressurization patterns for Group L and R tube propulsion, respectively. **c** is a motion of the device tip with Group L pressurization. **d** and **e** Motions driven by Group L and R tubes. The devices form left- and right-handed helices, which generates a right- and left-handed trajectories, respectively

A strategy for in-pipe steerable locomotion

Fundamental principles of six braided-tube device

As was mentioned in Chapter 1, a six braided-tube locomotive device, which is proposed in the previous work [33], comprises three tubes that are twisted to form left-handed helices, and three tubes twisted to form right-handed helices; L1, L2, and L3 in Fig. 1b denote the left-handed tubes, and R1, R2, and R3 in Fig. 1c denote the right-handed tubes. These tubes are arranged symmetrically and periodically.

In this section, we discuss the respective pressurizing patterns for single-direction helices, three left-handed tubes (Fig. 2a), and three right-handed tubes (Fig. 2b). Figure 2c, which focuses on the tip of the device, illustrates how periodic pressurization and depressurization of the three left-handed tubes generates motion. The pressurized tube inflates, is shifted to the outside of the device, and comes into contact with the inner wall of a pipe. When the tube is depressurized as the neighboring tube is pressurized, the device generates a rotation, rolls along the inner wall, and moves forward. When the rolling is propelled by the left-handed tubes, the device always forms a left-handed helix, which generates a right-handed trajectory, as is shown in Fig. 2d; the opposite situation is illustrated in Fig. 2e. As previously mentioned, the device can move backwards owing to a reverse pressurizing pattern; this movement occurs independent of the helical direction of tube inflation. Table 1 details the respective relationships between tube direction, locomotion, and rotation with respect to the tip of the device.

Since the direction of rotation is dependent on the direction of helices that the tubes form, we confirmed that pressurizing patterns, which utilize both helices, enable independent control of locomotion and rotation (Fig. 3a, b, respectively).

Figure 3 also illustrates the deformation that occurs when we change the direction of tube inflation. For example, we consider the deformation in the following procedure. Initially, L3, which is one of the left-handed tubes, inflates (Fig. 3c); the inflated L3 tube then comes into contact with the inner wall of a pipe and changes the shape of the device into a left-handed helix that runs parallel to L3. Then, R3, which is one of the right-handed tubes, inflates (Fig. 3d). When left- and right-handed

Table 1 Relationships between helical direction, locomotion, and rotation

	Forward	Backward
Group L tubes	CCW	CW
Group R tubes	CW	CCW

CW and CCW: clockwise and counterclockwise, respectively

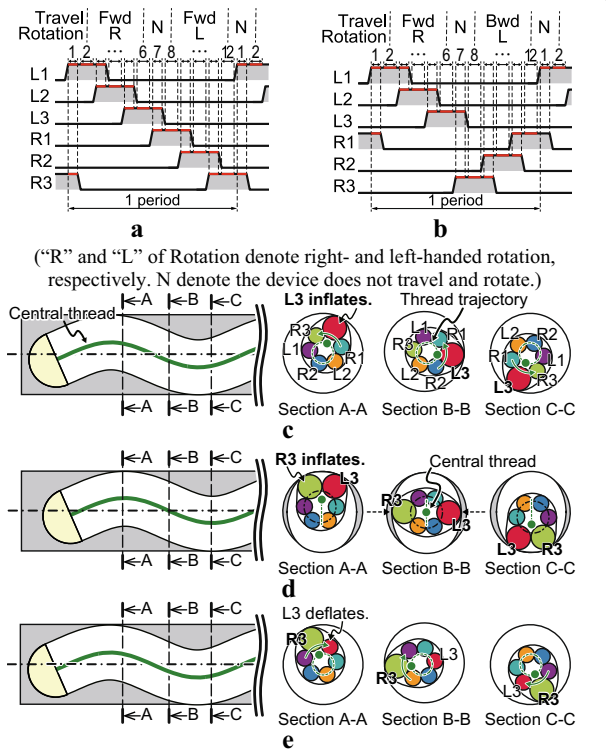

Fig. 3 Motion of six braided-tube device utilizes both groups of tubes. **a** and **b** Pressurizing patterns which generate only propulsion and rotation, respectively. With **a** pattern, the device travels in same direction and rotate in both directions, the propulsion exists while the rotations are canceled out. On the other hand, the rotation exists while the propulsion are canceled out with **b** pattern. **c**, **d**, and **e** The deformations when a tube of Group L (L3), one tube in each group (L3&R3), and a tube of Group R (R3) inflate, respectively. The device deforms into a left-handed helix, a planar wave, and a right-handed helix in **c**–**e**, respectively

tubes are simultaneously inflated, the two inflated tubes move in same directions along the same cut plane A–A, while they move in opposite directions and cancel out each deformation along the cut plane B–B. As we described before, the device bends with an inflation force of a tube. When both the right- and left-handed tubes inflate, we can consider the inflations of the tubes as the combined inflation of a tube. Because of the plane symmetry of the helical tubes, which have different directions and the same pitch and radius, the inflation of the tubes cancel each other and deform in a direction perpendicular to the plane of symmetry. We can treat this situation as if we are inflating a virtual tube, whose shape is similar to a planar wave.

Since the inflated tubes have a symmetrical arrangement, the tubes deform the device such that it resembles a planar wave (Fig. 3d). Finally, L3 deflates (Fig. 3e), changing the shape of the device into a right-handed helix (Fig. 3e), which is a planar symmetrical shape of the initial form (Fig. 3c). Thus, when the direction of inflated tubes is changed, the device does not move forward or backward, and the helical direction of the device is changed.

Strategy to select a branch

Based on the propulsion principles described above, we propose a new pressurizing pattern (Fig. 4a) that implements two left-handed and two right-handed tubes. Figure 4a illustrates the deformation pattern that generates motion. This pattern can be separated into four parts: Part 1 ($1 \rightarrow 2 \rightarrow 3$), Part 2 ($3 \rightarrow 4 \rightarrow 5$), Part 3 ($5 \rightarrow 6 \rightarrow 7$), and Part 4 ($7 \rightarrow 8 \rightarrow 1$). In Part 1, the state changes from only left-handed tube inflation to only right-handed tube inflation, and the direction of its helix is changed without generating locomotion. In Part 2, the right-handed tubes regulate the propulsion and rotation of the device. In Part 3, which is similar to Part 1, the direction of the helix is changed without generating locomotion. In Part 4, the left-handed tubes regulate propulsion and rotation. By repeating this pattern, we can propel the device forward and backward by using a reversed pattern.

As Fig. 4b shows, the range of motion of the tip of the device is limited; this is because the tip of the device is pushed toward the upper part of a pipe as it travels. Therefore, this new pressurizing pattern propels the device while maintaining the position and orientation of its tip (Fig. 4c). With regard to propulsion speed, this pressurizing pattern comprises eight steps of deformations ($1 \rightarrow \ldots \rightarrow 8 \rightarrow 1$), four of which generate travel ($7 \rightarrow 8 \rightarrow 1$ and $3 \rightarrow 4 \rightarrow 5$), i.e., 50% of the deformations in a cycle generate travel. Alternatively, the cycle of a typical pressurizing pattern, which is shown in Fig. 3a, comprises twelve steps of deformations ($1 \rightarrow \ldots 12 \rightarrow 1$), eight of which generate travel ($2 \rightarrow \ldots \rightarrow 6$ and $8 \rightarrow \ldots \rightarrow 12$), i.e., 75% of the deformations in a cycle generate travel. Therefore, the percentage of one cycle of the proposed pattern that is devoted to propulsion equates to 67% of that of a typical pattern.

In this study, branching systems are classified as either "Type A" (Fig. 5a), which consists of a right-hand turn and left-hand turn, or "Type B" (Fig. 5b), which consists of a straight path and a single turn. As shown in Fig. 6, although a six braided-tube device that follows

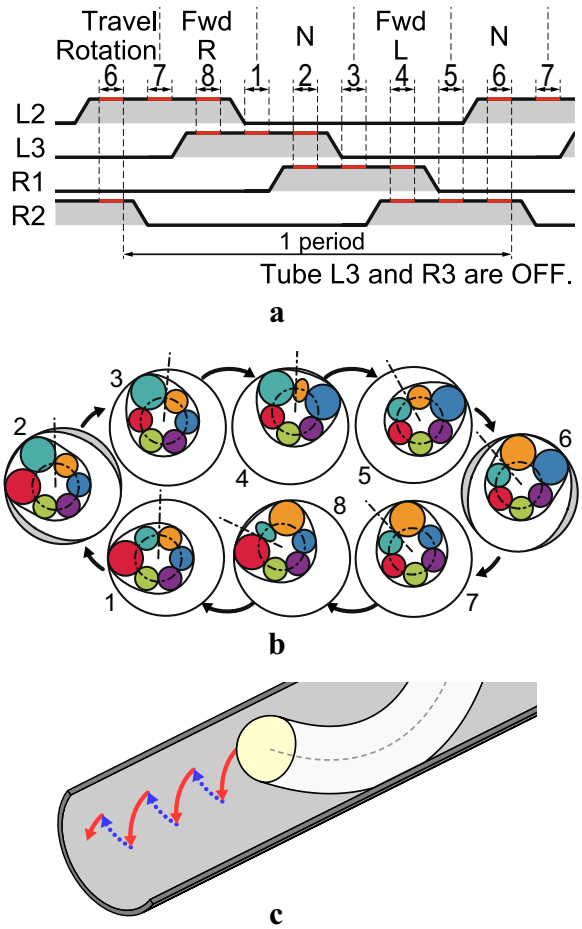

Fig. 4 Four-tube-driven locomotion with a steering hook. **a**–**c** The pressurization pattern for four-tube travel, the deformation of the device driven by four tubes, and the locomotion trajectory driven by four tubes. In **c**, the device switches a travel trajectory between a right-handed helix (a red and solid arrow) and a left-handed helix (a blue and dotted arrow)

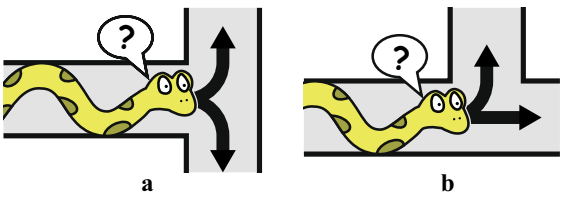

Fig. 5 Two branching system types. Type A (**a**) and Type B (**b**). Type A includes a 180° fork, and Type B includes a straight path and a branched path

the proposed pattern can select a path in Type A, it is unable to select a path in Type B. Thus, to ensure that a six braided-tube device can perform path selection in

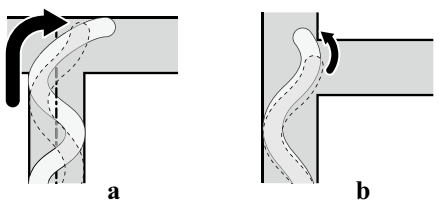

Fig. 6 Locomotion trajectory based on the locomotion pattern illustrated in Fig. 5. In Type A (**a**), the device is deformed by pressing itself against the inner wall of the desired branched pathway. In Type B (**b**), the device cannot hook into the inner wall of a branched pathway

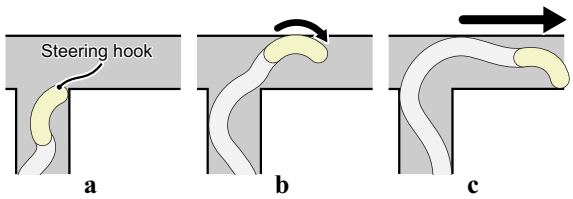

Fig. 7 Strategy for right-hand turns at Type A branch. **a** Device approaches the end of the pipe, keeping the tip of the device turned to the right. **b** Tip of the device comes into contact with the end of the pipe, causing it to bend rightward. **c** Tip enters the right branched pathway, with the device following. This strategy also enables left-hand turns with 180° rotation

both types of branching systems, steering attachments must be added. Although we could implement a previously developed steering mechanism with a few DoFs [23, 24], these mechanisms require an additional power supply and inevitably increase device complexity. Thus, we determined that the combination of a six-tube device and various pressurizing patterns would yield enough DoFs to enable path selection.

We propose an attachment referred to as a steering hook to allow a six-braided tube device to steer in a branched piping system, which is fabricated with rigid plastic and attached at the tip of the device. Figures 7, 8 and 9 show steering maneuvers made by the proposed steering hook. Rotation constrains the orientation of the hook, allowing the device to utilize the novel pressurizing pattern shown in Fig. 4a to maneuver the hook into a branched section. Thus, a combination of the hook and the various pressurizing patterns enables locomotion (Fig. 3a) and rotation (Fig. 3b), and the hook insertion (Fig. 4a) pattern enables the selection of the correct path in branched piping systems.

Figure 7 illustrates how the device maneuvers into a selected path in Type A. In Fig. 7a, the device is approaching a branch, making sure to keep the hook facing the path toward which the device will proceed.

Then, the hook makes contact with the inner wall and bends the device to proceed into the pathway (Fig. 7b). Finally, the device successfully passes the branch-off point and enters the pathway (Fig. 7c). Note that, if the device rotates 180 degrees before it approaches the branched path, the device can proceed toward an opposing path.

Figures 8 and 9 show how path selection and device maneuvering occurs in Type B. In Fig. 8, the device attempts to enter a branched path. Initially, the device approaches the branched pathway, keeping the hook facing the potential pathway (Fig. 8a). As the pressurizing pattern, which is shown in Fig. 4, causes the device to push the hook against the inner wall, the device can maneuver the hook into the branched pathway when it is within reach (Fig. 8b). The device can then be led into the branched pathway through the hook (Fig. 8c). On the other hand, Fig. 9 illustrates how the device travels along a straight path. As can be seen, the tip of the steering hook is angled away from the branched pathway such that the back of the steering hook repels off of the entrance corners of the branched pathway, thereby preventing the hook from entering and allowing the device to continue on a straight path. As discussed in this chapter, the combination of a six-braided tube device with a steering hook and the proposed pressurizing patterns realizes path selection in both types of branches.

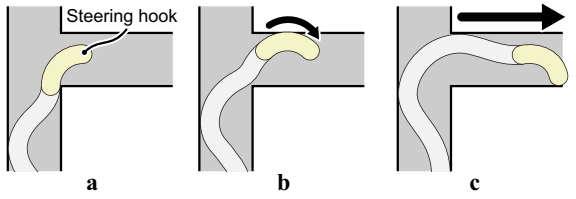

Fig. 8 Strategy for maneuvering the steering hook into a branched pathway at Type B branch. **a** Device approaches a branch, keeping the steering hook facing the branch. **b** Steering hook catches a corner of the branch, allowing it to enter the branched pathway. **c** Device follows the steering hook into the branch

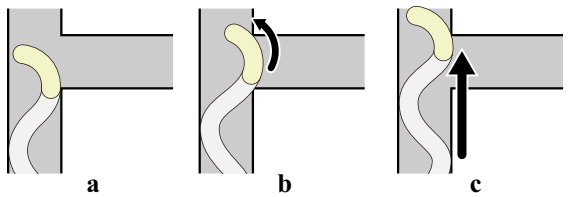

Fig. 9 Strategy for bypassing Type B branch. **a** Device approaches a branch, keeping the hook facing away from the branch. **b** Because the hook faces a wall that is opposite to the branch, the hook does not catch the branch. **c** Device does not turn

Prototypes and experimental equipment

Two prototypes of six braided-tube device

This chapter describes experimental implementation of two prototypes to evaluate the proposed propulsion and steering principles described in Chapter 2. We constructed two prototypes, which are shown in Fig. 10a, b; Prototype 1 has no steering hook and Prototype 2 has a steering hook. Silicone tubes made of KE-1416 (Shin-Etsu Chemical Co., Ltd.) with inner and outer diameters of 1.5 mm and 2.5 mm, respectively, were used to fabricate both prototypes. Following the fabrication method used in a previous study [33], we braided and glued the tubes around a nonstretchable thread so that the initial helical pitch p_{h0} is 45 mm and the tubes are placed as shown in Fig. 16d. Although the originally desired helical pitch was 45 mm, the actual helical pitches of Prototypes vary from 40 mm to 45 mm.

Prototype 1 includes a hemisphere cap made of acrylonitrile butadiene styrene (ABS) plastic. Additionally, there is a line indicator on the tip of the cap to indicate the device angle.

Alternatively, the steering hook, which Prototype 2 equips, must be sufficiently large to bypass a branched pathway and sufficiently small so as to not hinder propulsion in a straight pipe. The previous study shows that an upper limit of the inner diameter of a pipe through which the helical device can navigate is greater than $D_{d0} + p_{\mathrm{h0}}/2\pi$, where D_{d0} and p_{h0} denote the initial outer diameter of the device and the initial helical pith, respectively. Therefore, we can predict that the upper limit of the prototypes is 16 mm. Based on the above discussion, we use a pipe with an inner diameter of 14 mm. Therefore, we designed the steering hook as illustrated in Fig. 10c, for compatibility with a pipe with a 14-mm inner diameter. As shown in Fig. 10d, the axial hole in the steering hook can keep the core thread at the center of a device. We can implement a camera module in the device with the axial hole in a future work.

Experimental equipment

Figure 11 outlines the experimental system, which includes a personal computer (PC), an interface board, a pneumatic pressure regulator, pneumatic solenoid valves, and a prototype. The solenoid valves that connect to the prototype via silicone connection tubes, which do not inflate with a pneumatic pressure, can control the state (i.e., pressurized or depressurized) of each tube of the prototype. The pneumatic regulator regulates pressure which is used to pressurize/depressurize the tubes. The PC sends a pressurizing pattern to an interface board that controls the valves by command.

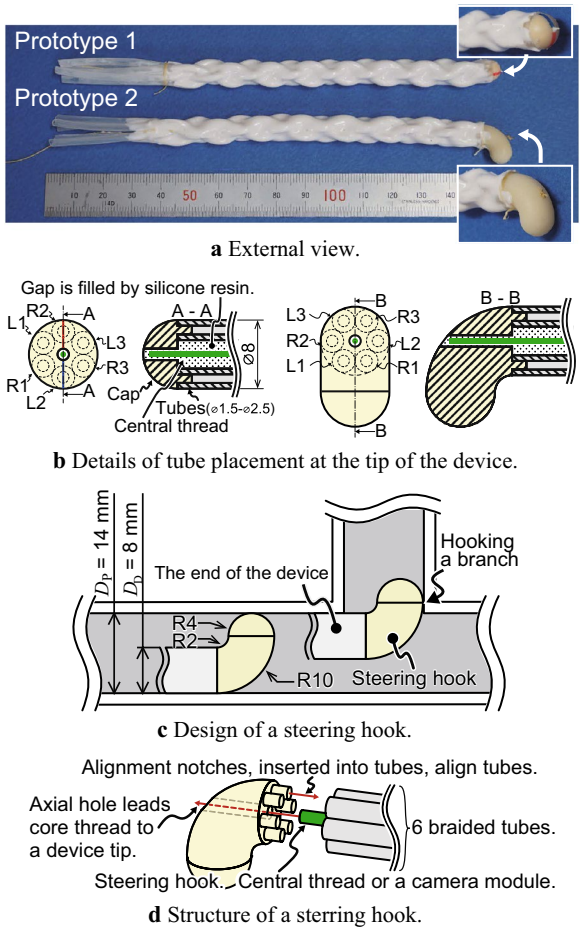

a External view.

b Details of tube placement at the tip of the device.

c Design of a steering hook.

d Structure of a sterring hook.

Fig. 10 Prototypes

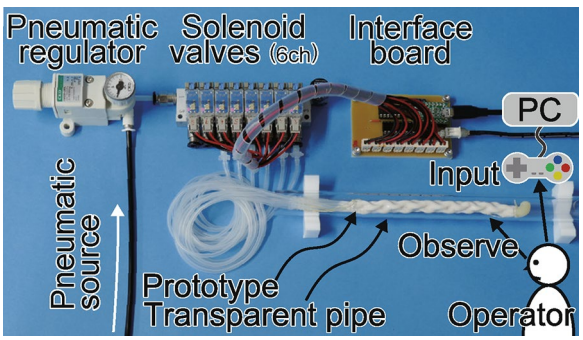

Fig. 11 Control system

Figure 12 shows the piping system, which comprises three pieces of a polymethyl methacrylate (PMMA) plastic pipe that was used to evaluate the performance of the prototypes. The arrows in Fig. 12 denote the A-type branch (Fig. 5a), B-type branch (Fig. 5b), and fork intersection (C-path in Fig. 12). Therefore, we can test the prototype in various branch types with the PMMA piping systems. Note that the prototypes were not equipped with a camera; thus, device movement was controlled based on an external view of the pipe.

Experiments

Straight-pipe locomotion experiment

A straight-pipe locomotion experiment was conducted to test the novel pressurizing pattern (Fig. 4b), and the utility of the steering hook of Prototype 2. Thus, to evaluate the pressurizing pattern and steering hook, both prototypes were driven through a straight segment of the piping system by using the pressurizing pattern shown in Fig. 3a, and that shown in Fig. 4b. Table 2 lists the propulsion speed per cycle of pressurization.

As was mentioned in "Strategy to select a branch" section, and as can be ascertained from Table 2, the speed achievable with four tubes (Fig. 4b) is nearly one half of that which can be achieved with six tubes (Fig. 3a). Table 2 also shows that the speed difference between prototypes with and without a hook is 20%.

From Fig. 13, which illustrates a cycle of motion of the device tip, it can be seen that the device is able to move forward while maintaining the position and orientation of the tip within a certain range. This confirms that the proposed method enables forward propulsion via a push-off mechanism by which the steering hook pushes off of the inner wall to propel forward.

To confirm the effect of a hook on traction force, we measure the climbing speed of both prototypes against some gravity forces. As shown in Fig. 14a, an external load is applied to a prototype through M8 nut. The weights of Prototypes A and B and the nut are 6 g, 6 g, and 4.5 g, respectively. Figure 14b shows the relationships between the measured speeds and applied loads. Both results of Prototypes A and B are the average of speeds obtained by performing two measurements on the two prototypes, and the error bars represent the maximum and minimum speeds. Because both the speeds and loads are respectively divided by the speed and load when a device lifts up only its body, both axes have no dimensions. As the measured result shows that the hook does not affect the relationship between loads and speeds, we confirmed that a hook does not affect the traction force of a device and both devices can lift objects that are heavier than themselves.

Steering experiments

We tested the steering capability of Prototype 2 in the test piping system shown in Fig. 12. Figure 15a shows how Prototype 2 can be steered through the A-type branched pipe; it can be seen that, when the prototype approaches the branch, the steering hook was turned toward the branch, thereby allowing the device to enter the pathway.

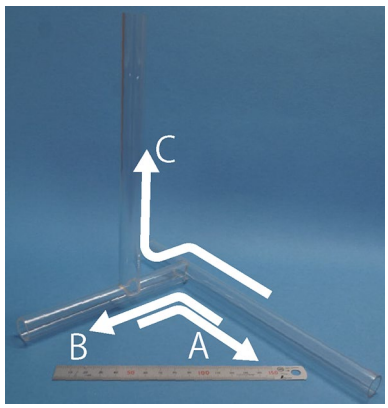

Fig. 12 Experimental PMMA piping system

Table 2 Locomotion speed in a straight pipe

	Prototype 1 (without a hook)	Prototype 2 (with a hook)
6 tubes	3.4 mm/cycle	2.9 mm/cycle
4 tubes	1.6 mm/cycle	1.3 mm/cycle

Secondly, the ability of Prototype 2 to bypass a branch and continue straightforward movement was also evaluated in the B-type branch. In this experiment, as is shown in Fig. 15b, the steering hook was turned away from the branched pathway as it passed, allowing the device to continue traveling forward.

Finally, the ability of Prototype 2 to proceed through two B-type branches was evaluated. Although the orientations of the two branches are different, the prototype is able to appropriately rotate the hook to allow it to enter each branched pathway.

These experimental results demonstrate that using a steering hook allows an operator to successfully steer the six braided-tube locomotive device through various types of branched pipes.

To confirm the success rate and time required for selecting a path, we measure the time required to move from the "Start" line to the "Finish" line. The experimental setups are shown in Fig. 16a–c. The setups that are shown in Fig. 16a, b evaluate the effect of a branch type because both setups comprise different types of branches but have the same direction. The setups that are shown in Fig. 16b, c evaluate the effect of gravity because both the setups comprise the same type of branch and gravity strongly prevents and helps in achieving hooking. In the experiments, we found that a prototype with a hook often achieves a stable state, which is shown in Fig. 16d. In this state, as the traction force of a device and the reaction force acting on the hook from an inner wall are balanced, the prototype stacks for a while. Therefore, in order to hook to a branch, the prototype initially moves in a hook-insertion pattern and reaches a stable state. Then, the

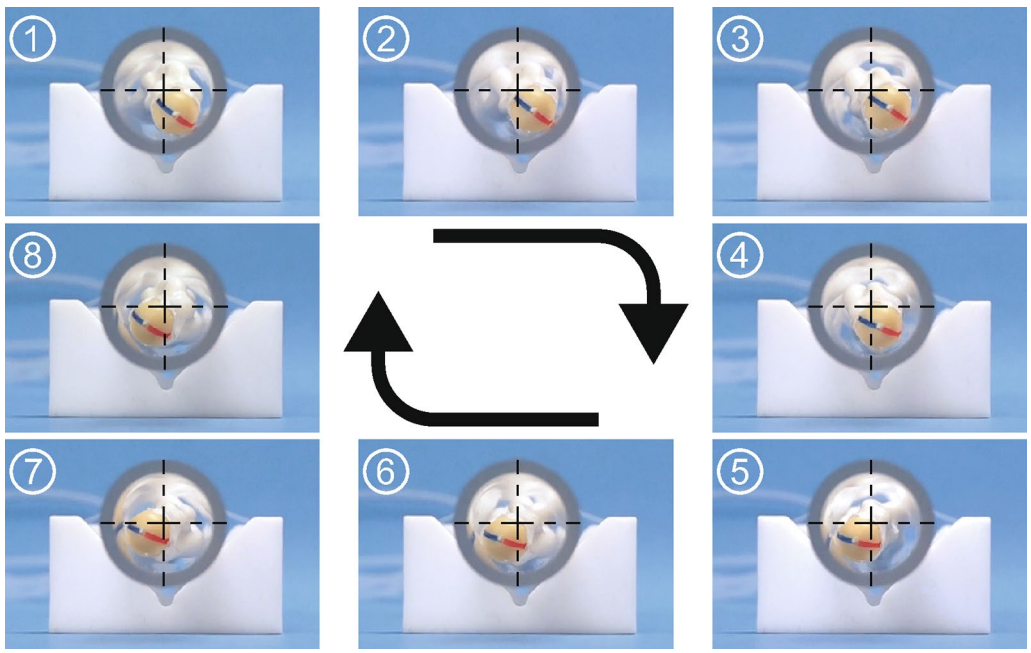

Fig. 13 Progression of Prototype 1 tip motion. The tip remains in the bottom-half of the pipe

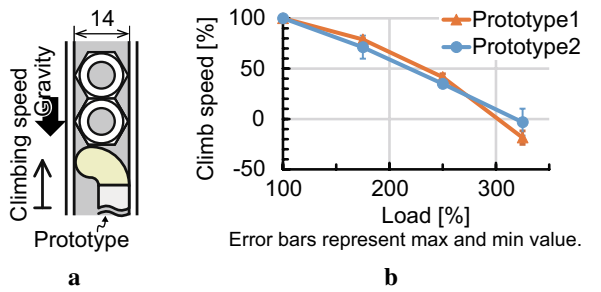

Fig. 14 Measurement of traction forces with both prototypes. **a**, **b** The experimental setup and measured results, respectively. The load values and speeds are obtained by $100\left(1 + N \cdot m_N/m_p\right)$[%] and $100(v/v_0)$[%], respectively, where m_p and m_N denote the weight of the prototype and M8 nut, respectively, N is the number of nuts, and v and v_0 denote the climbing speed with nuts and without nut

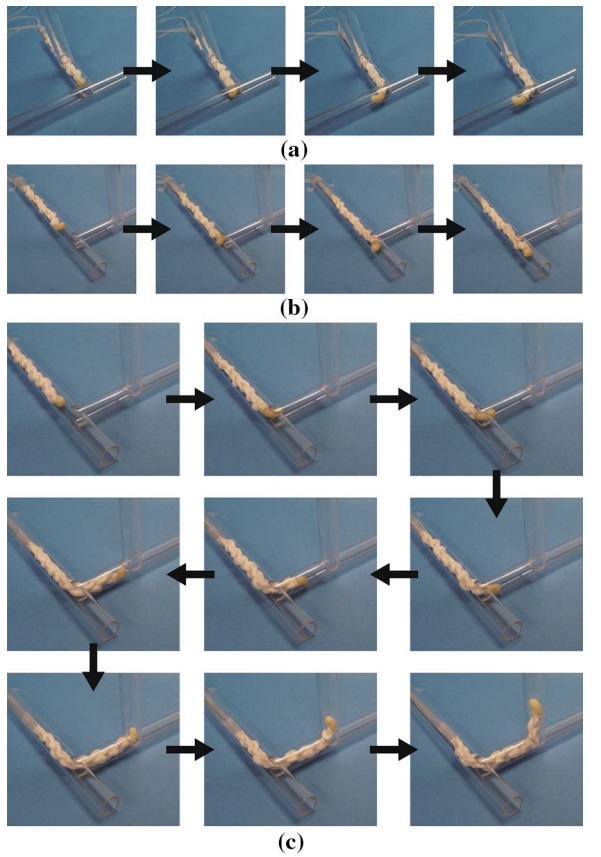

Fig. 15 Steering through the experimental piping system. A video of the experiment is available in Additional file 1. **a** Steering motion in an A-type branch (Path A in Fig. 12). **b** Straight locomotion in a B-type branch (Path B in Fig. 12). **c** Steering motion in skew branches (Path C in Fig. 12)

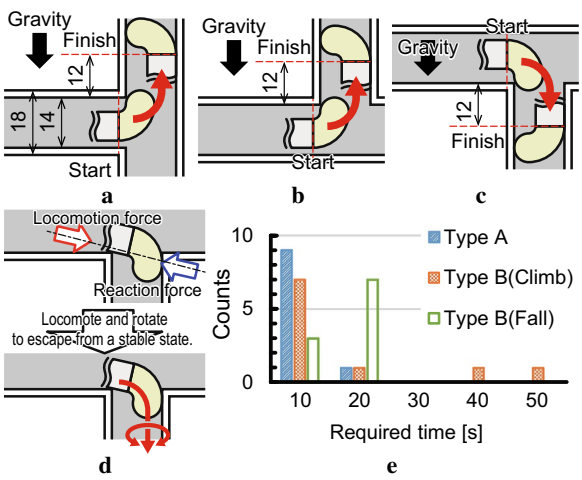

Fig. 16 Time required to pass through a branch. **a**–**c** The experimental setups. **d** The results

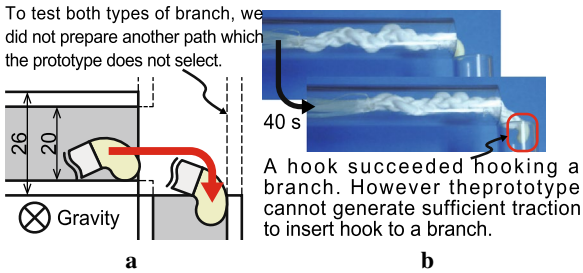

Fig. 17 Hooking experiment in a large pipe in which a prototype cannot move regularly. **a** The experimental setup. **b** The result

type of locomotion switches to helical rotation so that the prototype can escape from the stable state. Figure 16e shows the result of ten trials with each setup. Prototype 2 succeeded in entering a branch without any mistake nine, seven, and ten times in the setups shown in Fig. 16a–c, respectively. The averages and standard deviations of the time required are 11.0 s and 1.8 s, 11.9 s and 1.1 s, and 16.0 s and 2.5 s for the setups shown in Fig. 16a–c, respectively. These results show that gravity prevents the hook from hooking to a branch. However, a device can succeed in selecting a branch even though gravity disturbs a device, and the direction of gravity does not affect a required time.

To confirm that a steering hook can hook to a branch in pipes that have varying inner diameters, we consider the diameter range within which a hook can achieve hooking. A preliminary experiment shows that prototype 2 can move in pipes with inner diameters varying from 14 to 18 mm, the lower limit of which is limited by the shape of the hook and the upper limit is greater than that predicted in "Two prototypes of six braided-tube device" section. Therefore, we tested the device in

a pipe with an inner diameter of 20 mm, which is too large for the prototype to move because of a lack of traction. The experimental setup and results are shown in Fig. 17. We can confirm that the hook can achieve hooking in a large pipe in which a traction force of a prototype lacks. Therefore, the range of the inner diameter of a pipe through which a prototype can navigate is not limited by the range of the inner diameter within which a hook can achieve hooking but by the range of the traction force necessary to achieve locomotion.

Conclusion

As was described in Chapter 4, the proposed pressurizing pattern and prototypes enable successful path selection in branched piping systems. Moreover, the proposed pressurizing pattern, which was presented in "Strategy to select a branch" section, enables precisely regulated movement of the six braided-tube device, as shown in Fig. 13. Thus, the proposed pressurizing pattern implemented in the device with the proposed design of the steering hook enables successful path selection in branched piping systems.

As previously mentioned, the prototypes developed in this study were not equipped with a camera. In practical use, it is important to control the device from the viewpoint of a camera that is attached to the device. Therefore, in the future, we will attempt to attach a camera to the tip of the six braided-tube locomotive device to confirm controllability. Because we predict that the view of a camera attached at the tip of the device will be shaken by a motion of the tip, we must develop an image stabilizing method for the proposed device. We plan to synchronize an image update and a pressurizing pattern so that the view is updated with same device shape.

Additional file

Additional file 1. Path selection of a six braided-tube locomotive device with steering hook.

Abbreviations

FWD: forward; BWD: backward; CW: clockwise; CCW: counter-clockwise; PMMA: polymethyl methacrylate.

Authors' contributions

HT proposed a novel steering manner of the proposed mechanism and confirm it by the examinations. TT invented the proposed locomotive device and improved a quality of principles. Both authors read and approved the final manuscript.

Author details

[1] Tokyo Institute of Technology, 4259, Nagatsutacho, Midori-ku, Yokohama-shi, Kanagawa 226-0026, Japan. [2] Osaka University, 2-1, Yamadaoka, Suita-shi, Osaka 565-0871, Japan.

Acknowledgements

Not applicable.

Competing interests

The authors declare that they have no competing interests.

Availability of data and materials

Data sharing is not applicable to this article as no datasets were generated or analyzed during the current study (Additional file 1).

Funding

This work was supported by JSPS KAKENHI under Grant No. JP17K06253.

Publisher's Note

Received: 14 September 2018 Accepted: 3 December 2018
Published online: 11 December 2018

References

1. Bray DE, McBride D (1992) Nondestructive testing techniques. Wiley, New York
2. Ong PS, Anderson WL, Cook BD, Subramanyan R (1994) A novel X-ray technique for inspection of steel pipes. J Nondestruct Eval 13(4):165–173
3. Siqueira MHS, Gatts CEN, Da Silva RR, Rebello JMA (2004) The use of ultrasonic guided waves and wavelets analysis in pipe inspection. Ultrasonics 41(10):785–797
4. Brett CR, de Raad JA (1996) Validation of a pulsed eddy current system for measuring wall thinning through insulation. In: Proceedings of SPIE—the international society for optical engineering 2947(November):211–222
5. Okada T, Sanemori T (1987) MOGRER: a vehicle study and realization for in-pipe inspection tasks. IEEE J Robot Autom 3(6):573–582
6. Suzumori K, Miyagawa T, Kimura M, Hasegawa Y (1999) Micro inspection robot for 1-in pipes. IEEE/ASME Trans Mechatron 4(3):286–292
7. Kakogawa A, Ma S, Hirose S (2014) An in-pipe robot with underactuated parallelogram crawler modules. In: Robotics and automation (ICRA), 2014 IEEE international conference on 1687–1692
8. Kim HM, Choi YS, Lee YG, Choi HR (2016) Novel mechanism for in-pipe robot based on multi-axial differential gear mechanism. IEEE/ASME Trans Mechatron 22(1):227–235
9. Singh A, Sachdeva E, Sarkar A, Krishna KM (2017) COCrIP: compliant omniCrawler in-pipeline robot. In: Intelligent robots and systems (IROS), 2017 IEEE/RSJ international conference on 5587–5593
10. Ye C, Liu L, Xu X, Chen J (2015) Development of an in-pipe robot with two steerable driving wheels. In: 2015 IEEE international conference on mechatronics and automation (ICMA) 1955–1959
11. Nishimura T, Kakogawa A, Ma S (2012) Pathway selection mechanism of a screw drive in-pipe robot in T-branches. In: 2012 IEEE international conference on automation science and engineering (CASE) 25(2):612–617
12. Debenest P, Guarnieri M, Hirose S (2014) PipeTron series—robots for pipe inspection. In: Proceedings of the 2014 3rd international conference on applied robotics for the power industry 1–6
13. Oya T, Okada T (2005) Development of a steerable, wheel-type, in-pipe robot and its path planning. Adv Robot 19(6):635–650
14. Kataoka M, Kimura H, Inou N (2013) Hermetically-sealed flexible mobile robot 'MOLOOP' for narrow terrain exploration. In: IECON 2013-39th annual conference of the IEEE industrial electronics society 4156–4161
15. Zin MRAM, Sahari KSM, Saad JM, Anuar A, Zulkarnain AT (2012) Development of a low cost small sized in-pipe robot. Procedia Eng 41:1469–1475
16. Yaguchi H, Izumikawa T (2013) Wireless in-piping actuator capable of high-speed locomotion by a new motion principle. IEEE/ASME Trans Mechatron 18(4):1367–1376

17. Jeon W, Park J, Kim I, Kang YK, Yang H (2011) Development of high mobility in-pipe inspection robot. In: 2011 IEEE/SICE international symposium on system integration (SII) 479–484
18. Yanagida T, Adachi K, Yokojima M, Nakamura T (2012) Development of a peristaltic crawling robot attached to a large intestine endoscope using bellows—type artificial rubber muscles. In: 2012 IEEE/RSJ international conference on intelligent robots and systems 2935–2940
19. Yamamoto T, Konyo M, Tadokoro S (2015) A high-speed locomotion mechanism using pneumatic hollow-shaft actuators for in-pipe robots. In: 2015 IEEE/RSJ international conference on intelligent robots and systems (IROS)2015-Decem:4724–4730
20. Gilbertson MD, McDonald G, Korinek G, Van de Ven JD, Kowalewski TM (2017) Serially actuated locomotion for soft robots in tube-like environments. IEEE Robot Autom Lett 2(2):1140–1147
21. Qiao J, Shang J, Goldenberg A (2013) Development of inchworm in-pipe robot based on self-locking mechanism. IEEE/ASME Trans Mechatron 18(2):799–806
22. Mikawa A, Tsukagoshi H, Kitagawa A (2012) Tube actuator with drawing out drive aimed for the inspection in the narrow and curved path. In: 2010 IEEE/ASME international conference on advanced intelligent mechatronics 1368–1373
23. Kato S, Kato M, Ogawa S, Ono M (2004) Development of inchworm type mobile robot movable in pipes with T-junction. In: Proceedings of American Society for Precision Engineering 2004 Annual Meeting 257–260
24. Lim J, Park H, An J, Hong YS, Kim B, Yi BJ (2008) One pneumatic line based inchworm-like micro robot for half-inch pipe inspection. Mechatronics 18(7):315–322
25. Ozaki K, Wakimoto S, Suzumori K, Yamamoto Y (2011) Novel design of rubber tube actuator improving mountability and drivability for assisting colonosocope insertion. In: 2011 IEEE international conference on robotics and automation 3263–3268
26. Valdastri P, Webster RJ, Quaglia C, Quirini M, Menciassi A, Dario P (2009) A new mechanism for mesoscale legged locomotion in compliant tubular environments. IEEE Trans Robot 25(5):1047–1057
27. Nishikawa H et al. (1999) In-pipe wireless micro locomotive system. In: MHS'99. Proceedings of 1999 international symposium on micromechatronics and human science (Cat. No. 99TH8478) 141–147
28. Zagler A, Pfeiffer F (2003) 'MORITZ' a pipe crawler for tube junctions. In: 2003 IEEE international conference on robotics and automation (Cat. No. 03CH37422) 3:2954–2959
29. Takayama T, Takeshima H, Hori T, Omata T (2015) A twisted bundled tube locomotive device proposed for in-pipe mobile robot. IEEE/ASME Trans Mechatron 20(6):2915–2923
30. Mori M, Hirose S (2002) Three-dimensional serpentine motion and lateral rolling by active cord mechanism ACM-R3. Intell Robot Syst 2002. IEEE/RSJ Int Conf 1(October):829–834
31. Takeshima H, Takayama T (2017) Geometric estimation of the deformation and the design method for developing helical bundled-tube locomotive devices. IEEE/ASME Trans Mechatron 23(1):223–232
32. Takayama T, Hori T, Omata T (2011) Propelling principles for endoscope based on helical rolling motion and braid bending motion. J Jpn Soc Comput Aided Surg JJSCAS 13:246–247
33. Takeshima H, Takayama T (2015) Six-braided tube in-pipe locomotive device. In: 2015 IEEE/RSJ international conference on intelligent robots and systems (IROS) 2015–Decem:1125–1130